Measurement of Stimulated Hawking Emission in an Analogue System

Silke Weinfurtner,[1] Edmund W. Tedford,[2] Matthew C. J. Penrice,[1] William G. Unruh,[1] and Gregory A. Lawrence[2]

[1]*Department of Physics and Astronomy, University of British Columbia, Vancouver, Canada V6T 1Z1*

[2]*Department of Civil Engineering, University of British Columbia, 6250 Applied Science Lane, Vancouver, Canada V6T 1Z4*

(Received 30 August 2010; published 10 January 2011)

Hawking argued that black holes emit thermal radiation via a quantum spontaneous emission. To address this issue experimentally, we utilize the analogy between the propagation of fields around black holes and surface waves on moving water. By placing a streamlined obstacle into an open channel flow we create a region of high velocity over the obstacle that can include surface wave horizons. Long waves propagating upstream towards this region are blocked and converted into short (deep-water) waves. This is the analogue of the stimulated emission by a white hole (the time inverse of a black hole), and our measurements of the amplitudes of the converted waves demonstrate the thermal nature of the conversion process for this system. Given the close relationship between stimulated and spontaneous emission, our findings attest to the generality of the Hawking process.

DOI: 10.1103/PhysRevLett.106.021302 PACS numbers: 04.70.Dy, 04.60.−m, 04.62.+v, 47.35.Bb

One of the most striking findings of general relativity is the prediction of black holes, accessible regions of no escape surrounded by an event horizon. In the early 1970s, Hawking suggested that black holes evaporate via a quantum instability [1]. The study of classical and quantum fields around black holes shows that a pair of field excitations at temporal frequency f are created, with positive and negative norm amplitudes α_f, β_f (Bugoliubov coefficients) related by,

$$\frac{|\beta_f|^2}{|\alpha_f|^2} = \exp\left(\frac{-4\pi^2 f}{g_H}\right) \tag{1}$$

where $g_H = 10^{35}\ [\mathrm{kg/s}]/M$ is the surface gravity of the black hole with mass M [1,2]. Positive norm modes are emitted, while negative ones are absorbed by the black hole, effectively reducing its mass. A comparison of (1) with the Boltzmann-distribution allows one to associate a temperature T with the black hole, $T = 6 \times 10^{-8}\frac{M_\odot}{M}[\mathrm{K}]$, where $M_\odot$ is a solar mass, the smallest mass for an astrophysical black hole. Thus black hole evaporation is clearly difficult to observe directly [3].

In 1981 Unruh showed [4] (see also [3,5]), that there is a mathematical analogy between the behavior of classical and quantum fields in the vicinity of black hole horizons and sound waves in trans-sonic fluid flows and raised the possibility of doing experiments with these analogues. In 2002 Schützhold and Unruh argued that surface waves on an open channel flow with varying depth are a possible toy model for black hole experiments [6]. A difficulty with Hawking's derivation is its apparent reliance on arbitrarily high frequencies (the trans-Planckian problem [7–10]). The dispersion relation of gravity waves creates a natural physical short-wavelength cutoff, which obviates this difficulty. Thus the dependence of the Hawking effect on the high-frequency behavior of the theory can be tested in such analogue experiments [9]. While numerical studies indicate that the effect is independent of short-wavelength physics, experimental verification of this would strengthen our faith in the process. The presence of thermal emission in our physical system, which exhibits turbulence, viscosity, and nonlinearities, would indicate the generic nature of the Hawking thermal process.

The excitation spectrum of gravity waves on a slowly varying background flow is well understood and, neglecting surface tension and viscosity, has a dispersion relation given by $f^2 = (gk/2\pi)\tanh(2\pi kh)$, with the frequency $f = 1/\tau$, where τ is the wave period, the wave number $k = 1/\lambda$, where λ is the wavelength, g is the gravitational acceleration, and h the depth of the fluid. For $2\pi kh < 1$ the dispersion relation can be approximated by $f = \sqrt{gh}k$. These shallow water waves have both group and phase speed approximately equal to $\sqrt{gh}$. For $2\pi kh > 1$, the dispersion relation is approximated by $f = \sqrt{gk/2\pi}$. The group speed of these deep-water waves is approximately half the phase speed, both vary as the square root of the wavelength, and, for a given water depth, both are less than the speed of shallow water waves.

In [6] it was argued that the equation of motion of shallow water waves can be cast into a wave equation on a curved spacetime background if the speed of the background flow varies. Assuming a steady, incompressible flow, the velocity is $v(x) = q/h(x)$, where the two-dimensional flow rate per unit width q is fixed. The dispersion relation in the presence of a nonzero background velocity becomes $(f + vk)^2 = (\frac{gk}{2\pi})\tanh(2\pi kh)$. In Fig. 1, the dispersion relation is plotted for a flow typical of our experiments. Only the branch corresponding to waves propagating against the flow is plotted. For any linear field, where π is the conjugate momentum to ϕ, there is a conserved norm for complex solutions, $\langle\phi_1, \phi_2\rangle = \frac{i}{2} \times \int(\pi_1^*\phi_2 - \phi_1^*\pi_2)dx$, which has an indefinite sign. The

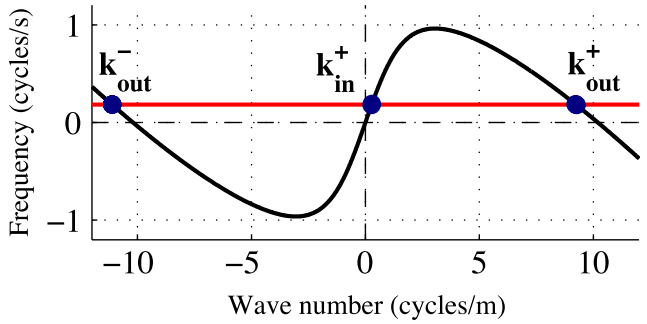

FIG. 1 (color online). Conversion process. Dispersion relation for waves propagating against a flow typical of our experiments. A shallow water wave, $k_{\rm in}^{+}$, sent upstream, is blocked by the flow and converted to a pair of deep-water waves ($k_{\rm out}^{+}$ and $k_{\rm out}^{-}$) that are swept downstream.

positive (negative) norm are associated with creation (annihilation) operators. For low frequencies, there are three possible waves, which we denote according to wave number. The first, $k_{\rm in}^{+}$, is a shallow water wave with both positive phase and group velocities, and also positive norm, and corresponds to the wave that we generate in our experiments. The second, $k_{\rm out}^{+}$, has positive phase velocity, negative group velocity, and positive norm. The third, $k_{\rm out}^{-}$, has both negative phase and group velocities, and lies on the negative norm branch. The second and third are both deep-water waves. In our experiment, the generated shallow water waves move into a region where they are blocked by an increasing countercurrent [11–14], and converted into the other two deep-water waves [15]. The goals of our experiment were to observe pair-wave creation, and to measure the relative amplitudes of the outgoing positive and negative norm modes to test the validity of Eq. (1).

It is this blocking of the ingoing waves that creates the analogy with the white hole horizon in general relativity. That is, there is a region that the shallow water waves cannot access, just as light cannot enter a white hole horizon. Note that while our experiment is on white hole horizon analogues, they are equivalent to the time inverse of black hole analogues.

Our experiments were performed in a 6.2 m long, 0.15 m wide and 0.48 m deep flume, and were partly motivated by experiments in similar flumes [11–14,16,17]. We created a spatially varying background flow by placing a 1.55 m long and 0.106 m high obstacle in the flume. This obstacle was modeled after an airplane wing with a flat top and a maximum downstream slope of 5.2° designed to prevent flow separation. We used particle image velocimetry [18] to determine q, and to verify the absence of flow separation. Shallow water waves of approximately 2 mm amplitude were generated 2 m downstream of the obstacle, by a vertically oscillating mesh, which partially blocked the flow as it moved in and out of the water. The intake reservoir had flow straighteners and conditioners to dissipate surface waves produced by the ingoing flow.

We measured and analyzed the variations in water surface height using essentially the same techniques as in [19]. A thin strip of the water surface was illuminated by a 0.5 W green (532 nm) laser light sheet created by a Powell lens. The water contained rhodamine-WT dye to create a sharp (< 0.2 mm) surface maximum in the fluorescence intensity which was photographed with a high-resolution (1080 p) monochrome camera. Each pixel corresponded to 1.3 mm on the water surface, the imaged area was 2 m wide and 0.3 m high, and the sampling rate was 20 Hz. We interpolated the intensity of light between neighboring pixels to determine the height of the water surface to subpixel accuracy (< 0.3 mm).

To detect the stimulated Hawking process, we sent shallow water waves toward the effective white hole horizon, which sits on the lee side of the obstacle. We conducted a series of experiments, with $q = 0.045$ m^2/s and $h = 0.194$ m, and examined 9 different ingoing frequencies between 0.02 and 0.67 Hz, with corresponding still water wavelengths between 69 and 2.1 m. This surface was imaged at 20 frames per second, for about 200 s. In all cases we analyzed a period of time which was an exact multiple of the period of the ingoing wave, allowing us to carry out sharp temporal frequency filtering of the signals (i.e., eliminating spectral leakage).

The analysis of the surface wave data was facilitated by introducing the convective derivative operator $\partial_t + v(x)\partial_x$. We redefine the spatial coordinate using, $\xi = \int_0 \frac{dx}{v(x)}$, where x is the distance downstream from the right-hand edge of the flat portion of the obstacle. The ξ coordinate has dimensions of time, and its associated wave number κ has units of Hz. The convective derivative becomes $\partial_t + \partial_\xi$, or, in Fourier transform space, $f + \kappa$. This is the term that enters the conserved norm. From Equations (35), (36) and (87) of Ref. [6] we find that the conserved norm has the form

$$\int \frac{|A(f,\kappa)|^2}{f+\kappa}\, d\kappa, \tag{2}$$

where $A(f, \kappa)$ is the $t - \xi$-Fourier transform of the vertical displacement of the wave. In using this coordinate system the outgoing waves have an almost uniform wavelength even over the obstacle slope.

We will illustrate the pair-wave creation process by presenting the results for $f_{\rm in} = 0.185$ Hz. Here we analyzed images from exactly 18 cycles, measuring the free surface along approximately 2 m of the flow including the obstacle. In Fig. 2(a) we plot the wave characteristics (amplitude as function of t and ξ) filtered to give only the temporal 0.185 Hz band. Figs. 2(b) and 2(c) are the characteristic plots where we further filter to include only $\kappa < -1$ Hz and $\kappa > 1$ Hz respectively. These are the negative and positive norm outgoing components without the central

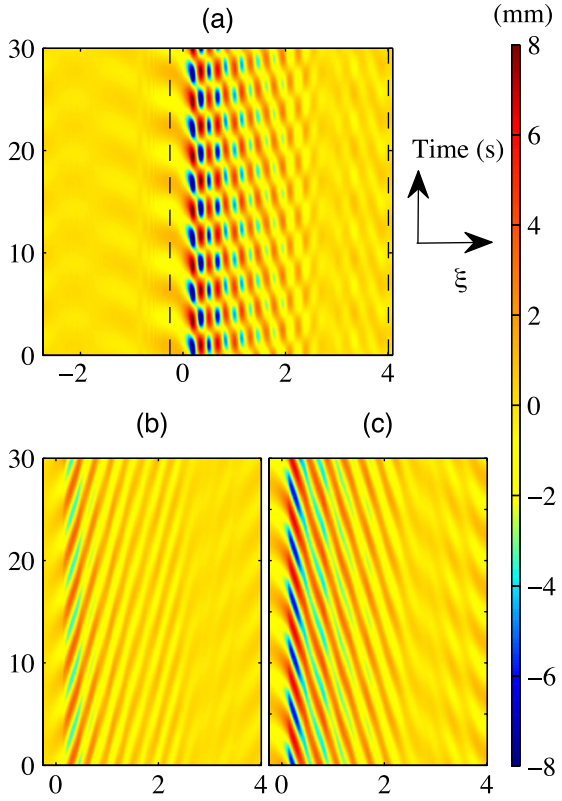

FIG. 2 (color online). Pair-wave creation. Demonstration of pair-wave conversion of an ingoing frequency of 0.185 Hz: (a) Filtered wave characteristic containing only the ingoing frequency band. (b) and (c) wave characteristics for filtered negative and positive norm modes. The colors represent the amplitudes of the waves; see color bars.

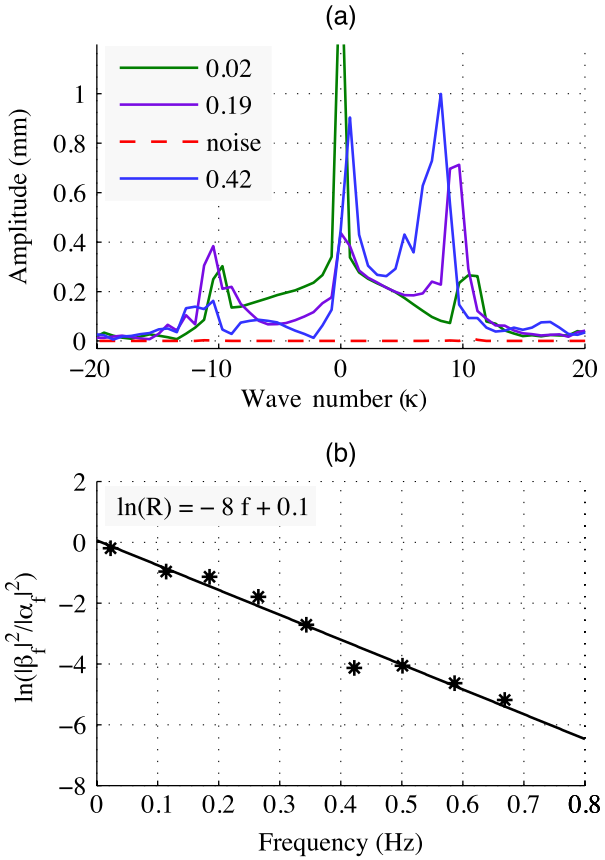

FIG. 3 (color online). Amplitudes and thermal spectrum. (a) Absolute value of three different ingoing frequency bands, and typical noise level (red line). (b) Natural log ratio R of negative and positive norm components [Eq. (1)] in between 0.02 and 0.67 Hz (black stars), and linear least-squares fit (black line).

peak of the ingoing wave (because of their very long wavelengths and the rapid change in wavelength as they ascend the slope, the incoming waves have a very broad Fourier transform). Recall that since we are only interested in counter-propagating waves, we defined positive phase and group speeds as pointing to the left. As expected from the dispersion relationship, see Fig. 1, the negative norm waves have negative phase velocity, while the positive norm waves have positive phase velocity. The complex structure in the characteristics of Fig. 2(a) arises because of the interference between the three components, the original ingoing wave and the positive and negative norm outgoing waves. In Fig. 2(c), we see that the ingoing wave is blocked around $\xi = 0$, with only a small component penetrating into the region over the top of the obstacle $\xi < 0$.

Our key results are presented in Fig. 3. Figure 3(a) shows the amplitude of the spatial Fourier transform at three selected ingoing frequencies. As the frequency increases, the ratio of the negative norm peak to positive norm peak decreases. Furthermore, the location of the positive norm peak moves slightly toward zero as the frequency increases, while the negative norm peak moves away from zero, as expected from the location of the allowed spatial wavenumber from the dispersion plot; see Fig. 1. The red curve in Fig. 3(a) shows the Fourier transform in the adjacent temporal frequency band for the sample case of 0.185 Hz. This is a representation of the noise, and is a factor of at least 10 lower than the signal in the 0.185 frequency band.

The crucial question is the following: Do the integrals of the negative to positive norm outgoing waves scale as predicted by the thermal hypothesis of Eq. (1)? This is shown to be the case in Fig. 3(b), where the norm ratios are plotted as a function of ingoing frequency. To evaluate $|\alpha_f|^2$ and $|\beta_f|^2$ we integrate $\int |A(f, \kappa)|^2/(f + \kappa) d\kappa$ over the respective peaks. In Fig. 3(b) the points represent the natural log of the ratios of these areas for each of the input frequencies we tested. The thermal hypothesis is strongly supported, with linear regression giving an inverse slope of 0.12 Hz and an offset close to zero. The slope corresponds to a temperature of $T = 6 \times 10^{-12}$ K.

We see from Figs. 2(b) and 2(c) that the region of "wave blocking", where the ingoing wave is converted to a pair of outgoing waves, is not a phase velocity horizon (where the phase velocity in the laboratory frame goes to zero) at this

frequency. The conversion seems to take place at the group velocity horizon (blocking) as noticed in Ref. [7]. This, together with the loss of irrotational flow near the horizon, and absence of a dependable theory of surface waves over an uneven bottom make prediction of the temperature from the fluid flow difficult. Our estimates give us a value somewhere between about 0.08 and 0.18 Hz. What is important is that the conversion process does exhibit the thermal form predicted for the Hawking process.

We have conducted a series of experiments which verified the thermal nature of the stimulated Hawking process at a white hole horizon in a fluid analogue gravity system. The thermal emission process is generic, it survives fluid-dynamical complications, such as turbulence and viscosity that are not part of the analogy. The ratio is thermal despite the different dispersion relation from that used by Hawking in his black hole derivation. It is thermal even though the ingoing frequencies do not experience a phase velocity horizon. However the in-going waves exhibit a group velocity horizon in this system, see Fig. 2, which is usually considered necessary, and as it seems sufficient, for the thermal effect. This increases our trust in the ultraviolet independence of the effect. When the thermal emission was originally discovered by Hawking, it was believed to be a feature peculiar to black holes. Our experiments, and prior numerical work [5,16], demonstrate that this phenomenon seems to be ubiquitous, and not something that relies on quantum gravity or Planck-scale physics.

While our experiments measure only the stimulated emission from this white hole analogue, it has been known since Einstein's work (see also Haus and Mullen [20]) that there is a very close relation between spontaneous and stimulated emission from a quantum system. For a linear system (which our small surface waves are), the classical behavior (amplification and Bugoliubov coefficients) completely determine the quantum behavior and quantum noise (which the Hawking radiation is). Furthermore, the time reversal invariance of the theory leads to the equivalence of black and white hole horizons. It would still be exciting to measure the spontaneous emission from a black hole. While finding small black holes to test the prediction directly is beyond experimental reach, such measurements might be achievable in other analogue models, like Bose Einstein condensates, or optical fibre systems [21–24].

We thank Mauricio Richartz for his help during the initial stages of this project. WGU and GAL thank the NSERC. WGU thanks the Canadian Institute for Advanced Research, and GAL thanks the Canada Research Chairs program. S. W. was supported by a MC Fellowship EMERGENT-2007-SW. We thank the Department of Civil Engineering for the use of the undergraduate flume and experimental space. Their willingness to make do with other equipment and space made our experiments possible.

[1] S. W. Hawking, Nature (London) **248**, 30 (1974).
[2] W. G. Unruh, Phys. Rev. D **14**, 870 (1976).
[3] C. Barceló, S. Liberati, and M. Visser, Living Rev. Relativity **8**, 12 (2005).
[4] W. G. Unruh, Phys. Rev. Lett. **46**, 1351 (1981).
[5] T. A. Jacobson and R. Parentani, Sci. Am. **17**, 12 (2007).
[6] R. Schützhold and W. G. Unruh, Phys. Rev. D **66**, 044019 (2002).
[7] W. G. Unruh, Phys. Rev. D **51**, 2827 (1995).
[8] T. Jacobson, Phys. Rev. D **53**, 7082 (1996).
[9] S. Corley and T. Jacobson, Phys. Rev. D **59**, 124011 (1999).
[10] M. Visser, Int. J. Mod. Phys. D **12**, 649 (2003).
[11] G. Rousseaux, P. Maïssa, C. Mathis, P. Coullet, T. G. Philbin, and U. Leonhardt, New J. Phys. **12**, 095018 (2010).
[12] I. K. Suastika, Ph.D. thesis Technische Universiteit Delft, The Netherlands, http://repository.tudelft.nl/view/ir/uuid:634218fc-e716-4bbc-9cd7-08221404fd34/, 2004.
[13] W. G. Unruh, Phil. Trans. R. Soc. A **366**, 2905 (2008).
[14] G. Rousseaux, C. Mathis, Philippe Maïssa, G. Thomas, and U. Leonhardt, New J. Phys. **10**, 053015 (2008).
[15] Further conversion from deep-water waves to capillary waves [11,16] are also possible but are not considered.
[16] S. T. Badulin, K. V. Pokazeyev, and A. D. Rozenberg, Izv. Atmos. Ocean Phys. **19**, 782 (1083).
[17] G. A. Lawrence, J. Hydr. Engrg. **113**, 981 (1987).
[18] R. J. Adrian, Annu. Rev. Fluid Mech. **23**, 261 (1991).
[19] E. W. Tedford, R. Pieters, and G. A. Lawrence, J. Fluid Mech. **636**, 137 (2009).
[20] A. Einstein, Phys. Z. **XVIII**, 121 (1917); H. A. Haus and J. A. Mullen, Phys. Rev. **128**, 2407 (1962).
[21] S. Dimopoulos, and G. Landsberg, Phys. Rev. Lett. **87**, 161602 (2001).
[22] P. Jain, A. S. Bradley, and C. W. Gardiner, Phys. Rev. A **76**, 023617 (2007).
[23] F. Belgiorno, S. L. Cacciatori, G. Ortenzi, V. G. Sala, and D. Faccio, Phys. Rev. Lett. **104**, 140403 (2010).
[24] B. J. Carr and S. B. Giddings, Sci. Am. **292**, 48 (2005).